

Crystallization of PDMS: The effect of physical and chemical crosslinks

This content has been downloaded from IOPscience. Please scroll down to see the full text.

2002 Europhys. Lett. 60 390

(<http://iopscience.iop.org/0295-5075/60/3/390>)

View [the table of contents for this issue](#), or go to the [journal homepage](#) for more

Download details:

IP Address: 132.72.9.170

This content was downloaded on 25/11/2014 at 09:50

Please note that [terms and conditions apply](#).

Crystallization of PDMS: The effect of physical and chemical crosslinks

T. DOLLASE^{1,2,3(*)}, H. W. SPIESS^{1,2}, M. GOTTLIEB^{1,3} and
R. YERUSHALMI-ROZEN^{1,3(**)}

¹ *The Reimund Stadler Minerva Center for Mesoscale Macromolecular Engineering*

² *Max-Planck-Institut für Polymerforschung - Ackermannweg 10
55128 Mainz, Germany*

³ *Department of Chemical Engineering, Ben-Gurion-University of the Negev
Beer-Sheva, 84105, Israel*

(received 22 April 2002; accepted 19 August 2002)

PACS. 61.25.Hq – Macromolecular and polymer solutions; polymer melts; swelling.

PACS. 68.35.Md – Surface thermodynamics, surface energies.

Abstract. – Calorimetric studies of the crystallization behavior of physically and chemically crosslinked semicrystalline polymer, polydimethylsiloxane (PDMS) are presented. Physical crosslinks are introduced either via entanglements in high-molecular-weight PDMS, or by anchoring chain ends to rigid polyethylene oxide (PEO) endblocks in a PEO-*b*-PDMS-*b*-PEO triblock copolymer. Chemical end-linking of di-vinyl PDMS chains results in the formation of a crosslinked network. Comparison of the thermograms obtained for each of these systems at constant cooling/heating rates with their noncrosslinked analogues indicates that, contrary to conventional wisdom, the different types of crosslinks result in an increased crystallization tendency. We suggest that this effect is a manifestation of the enhancement of local ordering together with reduced dynamics as compared to the non-crosslinked melt.

The effect of topological and geometrical constraints such as transient entanglements, chemical and physical crosslinks on the crystallization of polymers from the melt is practically important and scientifically interesting. It is well known that polymer crystallization upon cooling of a melt is controlled by kinetic considerations [1,2]. In the framework of the classical crystallographic models, the presence of constraints that reduce the mobility of the chains should lead to a reduction in the crystallization rate and result in a lower degree of crystallinity at a given cooling rate. Yet, experimental findings suggest that in several cases crystallization from the entangled melt is more efficient than that from the non-entangled analogue [3].

Recently, a conceptually different mechanism of “spinodal-like” crystallization was suggested [4–7]. In the framework of this model, crystallization is expected to occur via the evolution of correlated density and structural fluctuations. The process is cooperative, and crystallization proceeds via a preordered granular crystalline mesophase. These ideas have

(*) Present address: Tesa AG - Quickbornstraße 24, 20253 Hamburg, Germany.

(**) E-mail: rachely@bgumail.bgu.ac.il

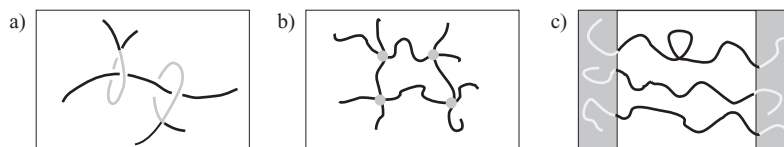


Fig. 1 – A schematic representation of a) entangled melt of polymers; b) a chemically crosslinked network of polymers; c) a triblock copolymer a-b-a where the two edge blocks are glassy at room temperature.

been supported by experimental observations [6, 7]. According to these concepts, regions that exhibit local ordering may facilitate the crystallization.

While geometrical and topological constraints are known to affect the dynamics of a melt [8, 9], it was suggested more recently that constraints can also lead to local ordering in globally amorphous polymer melts [10–13]. Rheological [9, 14], neutron scattering [15] and nuclear magnetic resonance (NMR) spectroscopy [16–18] approaches have been used to investigate these effects experimentally.

In this study we investigate the effect of topological and geometrical constraints on the crystallization of a simple semicrystalline polymer, polydimethylsiloxane, PDMS. Three types of crosslinks are examined: entanglements in PDMS homopolymers, endblocks which confine the central PDMS block in polyethyleneoxide-*b*-PDMS-*b*-polyethyleneoxide (PEO-*b*-PDMS-*b*-PEO) and chemical crosslinking of PDMS (fig. 1).

Differential-scanning calorimetry (DSC), which records heat flux changes as a function of time [19, 20], was used to follow the thermal behavior and in particular the crystallization kinetics of the different systems. Unless otherwise noted, experiments were carried at fixed cooling/heating rates of $\beta = \pm 5 \text{ K min}^{-1}$. All data are normalized with respect to the weight fraction of the corresponding type of polymer (PDMS or PEO).

PDMS samples: 5000 g mol^{-1} (United Chemical Technologies, denoted PDMS 5k), PDMS 16000 g mol^{-1} (PDMS 16k), PDMS $100000 \text{ g mol}^{-1}$ (PDMS 100k) were prepared by living anionic polymerization. PDMS 5k was end-linked, following Adam *et al.* [21], and is denoted x-PDMS 5k. The symmetric PEO-*b*-PDMS-*b*-PEO triblock copolymer was synthesized by Zhang [22]. The molecular weight of the PDMS center block is 12000 g mol^{-1} , the PEO fraction is 25% corresponding to a molecular weight of 2000 g mol^{-1} per PEO block. PEO/PDMS blends were prepared by mixing PDMS 12k (UTC) and PEO 2k (Clariant AG) at 100°C . The weight fraction of PEO in the blend is similar to that in the triblock copolymer (at room temperature the blend is in the two-phase regime).

A thermogram of PDMS 16k is presented in fig. 2 [8]. We regard PDMS 16k as effectively unentangled [8]. In agreement with other studies (for example, [23]) we find that following a cooling rate of $\beta = -5 \text{ K min}^{-1}$ the DSC thermograms of linear PDMS 16k exhibit upon heating a glass transition, T_g , and a complex melting pattern, particularly typical double melting peaks [24].

In this study we used three features as (dependent) markers for probing the crystallization behavior of PDMS: the presence (or absence) of the exothermal peak appearing during the cooling cycle, T_g , and the value of ΔH_c , the phase transition enthalpy related to the cold crystallization process.

We observed that linear non-entangled PDMS does not crystallize during the cooling sequence at cooling rates as low as $\beta = -1 \text{ K min}^{-1}$ [25]. Upon heating, the polymer crystallizes at T_c due to the reduction of melt viscosity. The latter enables chain rearrangements and leads to crystallization from the amorphous phase [2].

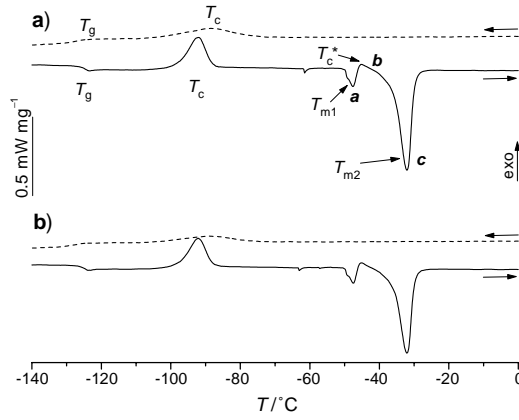


Fig. 2 – DSC thermograms of pure PDMS 16k, measured at a cooling/heating rate of $\beta = \pm 5 \text{ K min}^{-1}$. The dashed line is a cooling curve, the solid line a heating curve: a) first run; b) subsequent run. In the cooling curve we observe an exothermic peak T_c and a glass transition at T_g ($T_g = -127.9^\circ\text{C}$, $\Delta c_p = 0.19 \text{ J g}^{-1} \text{ K}^{-1}$). In the heating curve we observe a glass transition, T_g , an exothermic peak, the so-called cold crystallization, T_c ($T_c = -98.5^\circ\text{C}$, $\Delta H_{T_c} = +22.5 \text{ J g}^{-1}$), two melting peaks, T_{m1} (a) ($T_{m1} = 50.5^\circ\text{C}$, $\Delta H_{m1} = -4.1 \text{ J g}^{-1}$) and T_{m2} (c) ($T_{m2} = 34.0^\circ\text{C}$, $\Delta H_{m2} = -31.0 \text{ J g}^{-1}$), and a recrystallization exotherm, T_{c^*} (b) ($T_{c^*} = -47.4^\circ\text{C}$, $\Delta H_{T_{c^*}} = +2.2 \text{ J g}^{-1}$).

At a cooling rate $\beta = -5 \text{ K min}^{-1}$, PDMS 100k and x-PDMS 5k exhibit a sharp crystallization peak during the cooling scan (figs. 3a and b, respectively) while the non-entangled PDMS 5k (fig. 3c and table I) and PDMS 16k (fig. 2) do not. The heating curve of PDMS 5k is very similar to that of PDMS 16k (fig. 2). For both PDMS 100k and x-PDMS 5k, substantial crystallization takes place during cooling, suggesting a higher crystallization rate than that of PDMS 5k. Note that for PDMS 100k the presence of a shallow peak in the heating curve indicates that crystallization is not completed during cooling. The melting sequence of the crosslinked PDMS displays only a single melting peak: We suggest that due to the inability of crosslinks to crystallize, the distance between adjacent crosslinks determines the thickness of the crystalline lamellae and prevents rearrangements and crystallite thickening.

The thermal behavior of PDMS segments was also examined in three symmetric PEO-*b*-PDMS-*b*-PEO systems with 12000 g mol^{-1} PDMS center blocks and terminal PEO blocks

TABLE I – Numerical values of thermal transitions obtained by DSC for the PEO block as (temperatures in celsius) endblock in PEO-*b*-PDMS-*b*-PEO triblock copolymers (top); in PDMS/PEO polymer blends (bottom).

PEO blocks in triblocks	cooling curve	$T_c = -28.8$ $\Delta H_{T_c} = +8.5 \text{ J g}^{-1}$	
	heating curve	T_c non ΔH_{T_c} non	$T_{m1} = +48.3$ $\Delta H_{T_{m1}} = -13.4 \text{ J g}^{-1}$
PEO in blend	cooling curve	$T_c = +37.8$ $\Delta H_{T_c} = +10.1 \text{ J g}^{-1}$	
	heating curve	T_c n.o. ΔH_{T_c} n.o.	$T_{m1} = +52.6$ $H_{T_{m1}} = -13.4 \text{ J g}^{-1}$

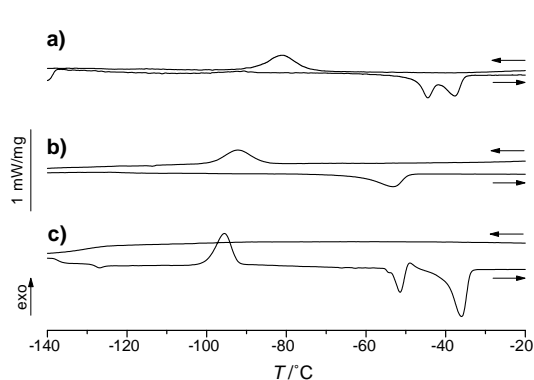


Fig. 3

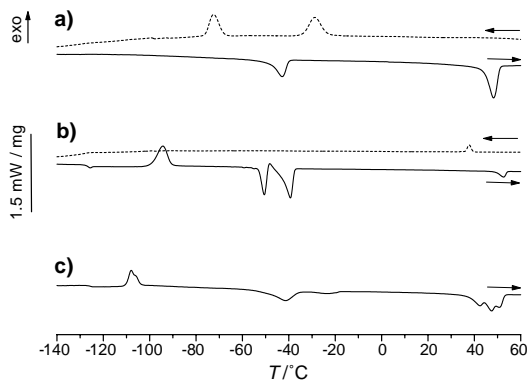


Fig. 4

Fig. 3 – DSC thermograms of PDMS measured at a cooling/heating rate of $\beta = \pm 5 \text{ K min}^{-1}$. a) PDMS 100k. b) Crosslinked polymer, x-PDMS 5k. c) The non-crosslinked precursor, PDMS 5k.

Fig. 4 – DSC thermograms measured at a cooling/heating rate of $\beta = \pm 5 \text{ K min}^{-1}$. a) 2k-12k-2k triblock copolymer (see numerical data in table II). b) A blend of PDMS 12k/PEO 2k with 28% weight fraction of PEO (table III). c) DSC thermogram of the 2k-12k-2k triblock copolymer measured at a heating rate of $\beta = +5 \text{ K min}^{-1}$ following quench cooling in liquid nitrogen.

of different chain length (550 g mol^{-1} , 2000 g mol^{-1} , 5000 g mol^{-1}). While the thermograms differed with regard to the PEO behavior, the thermal features of the PDMS block were similar. Here we focus on the 2k-12k-2k triblock copolymer. Numerical data are summarized in tables II and III. Figure 4a shows that the PDMS blocks crystallize readily under the applied cooling conditions. A blend of PDMS 12k/PEO 2k with a weight fraction of PEO equal to the one present in the triblock copolymer (28%) was used as a reference, fig. 4b.

The thermogram of the PDMS/PEO blend is a simple superposition of the DSC curves of the respective pure homopolymers indicating the absence of significant interactions between PEO and PDMS. In particular, PDMS does not crystallize during the cooling scan at a cooling

TABLE II – Numerical values of thermal transitions obtained by DSC for the PDMS block as (temperatures in celsius) center block in PEO-*b*-PDMS-*b*-PEO triblock copolymer (top); in PDMS/PEO polymer blends (bottom).

PDMS blocks in triblocks	cooling curve	T_g n.o. Δc_p n.o.	$T_c = -72.5$ $\Delta H_{T_c} =$ $+25.5 \text{ J g}^{-1}$			
	heating curve	T_g n.o. Δc_p n.o.	T_c n.o. ΔH_{T_c} n.o.	$T_{m1} = -42.9$ $\Delta H_{T_{m1}} =$ -27.7 J g^{-1}	T_c^* n.o. $\Delta H_{T_c^*}$ n.o.	T_{m2} n.o. $\Delta H_{T_{m2}}$ n.o.
PDMS in blend	cooling curve	$T_g = -126.0$ Δc_p n.o.				
	heating curve	$T_g = -128.0$ $\Delta c_p =$ $0.33 \text{ J g}^{-1} \text{ K}^{-1}$	$T_c = -94.3$ $\Delta H_{T_c} =$ $+25.2 \text{ J g}^{-1}$	$T_{m1} = -50.6$ $\Delta H_{T_{m1}} =$ -14.1 J g^{-1}	$T_c^* = -48.2$ $\Delta H_{T_c^*} =$ $+1.8 \text{ J g}^{-1}$	$T_{m2} = -39.4$ $\Delta H_{T_{m2}} =$ -26.4 J g^{-1}

TABLE III – Numerical values of thermal transitions obtained by DSC for the PEO block as (temperatures in celcius) endblock in PEO-*b*-PDMS-*b*-PEO triblock copolymers (top); in PDMS/PEO polymer blends (bottom).

PEO blocks in triblocks	cooling curve	$T_c = -28.8$ $\Delta H_{T_c} = +8.5 \text{ J g}^{-1}$	
	heating curve	T_c n.o. ΔH_{T_c} n.o.	$T_{m1} = +48.3$ $\Delta H_{T_{m1}} = -13.4 \text{ J g}^{-1}$
PEO in blend	cooling curve	$T_c = +37.8$ $\Delta H_{T_c} = +10.1 \text{ J g}^{-1}$	
	heating curve	T_c n.o. ΔH_{T_c} n.o.	$T_{m1} = +52.6$ $H_{T_{m1}} = -13.4 \text{ J g}^{-1}$

rate of $\beta = -5 \text{ K min}^{-1}$. Unlike the blend, PEO-*b*-PDMS-*b*-PEO exhibits two fairly sharp DSC features in the cooling scan, the crystallization exotherms of PEO and PDMS. In the heating scan neither a glass transition nor cold crystallization could be determined, but one melting peak for PDMS and one melting peak for PEO were observed.

Comparison of the corresponding thermograms suggests that while linear PDMS does not crystallize during the cooling scan down to a rate of $\beta = -1 \text{ K min}^{-1}$, PEO-*b*-PDMS-*b*-PEO crystallizes readily at a cooling rate of $\beta = -5 \text{ K min}^{-1}$. The heating run after quench cooling (in liquid nitrogen), fig. 4c, shows that the crystallization process of the PDMS block in the block-copolymer, can be suppressed under these conditions leading to vitrification of PDMS. Note that the crystallization of the PEO block in the triblock-copolymer is affected as well: During the cooling cycle the PEO block crystallizes at a lower temperature than in the blend. Yet, the degree of crystallization is greatly enhanced in the block copolymer as manifested by the magnitude of the crystallization and melting peaks (fig. 4, tables II, III).

The observation that topological and geometrical constraints enhance the crystallization rate of PDMS melts, may seem surprising at first sight, as constraints are believed to interfere with the crystallization process. However, polymer crystallization may be viewed as an ordering transition in which a small set of conformations becomes energetically favored, due to enthalpic considerations, leading to a severe reduction in conformational entropy. When crystallization is induced by rapid cooling the flexibility of the chains seriously diminishes, and the chains can only attain a limited ensemble of conformations separated by low activation energy barriers, rather than those of the lowest free energy. Thus, vitrification often dominates over crystallization. When the polymer melt is cooled at a slow enough rate, the probability of adopting the lowest-energy conformational state is increased, and some of the material can crystallize. If locally ordered regions are present in the melt, at elevated temperatures, the conformational space available to the melt chains is already reduced. While the specific type of order may not be that of the crystalline structure, the reduction in the total number of available conformations increases the probability of occupying the subset of conformations relevant to crystallizations. As long as the sub-set of conformations which lead to crystallization is not excluded, local ordering is expected to enhance crystallization. The elevated temperatures allow the system to span the reduced conformational space, and adopt the favored configurations over a shorter time period. In the case of PDMS, it may even be that the local organization of chains is lamellae-like resulting in a more specific enhancement of crystallization. This statement agrees with the key idea of the spinodal-like approach to polymer crystallization [4, 5].

In the following we discuss in detail the nature of the different constraints investigated

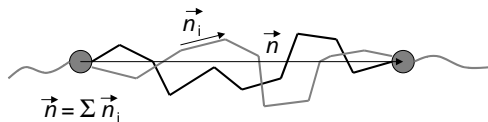


Fig. 5 – A schematic description of chain segments between two adjacent crosslinks.

in this study. Entanglements are topological constraints to chain dynamics that originate from intermolecular excluded-volume interactions [8,9]. Entanglements affect the mechanical properties [8,14] as well as the microscopic structure of amorphous polymers in the melt [16–18]. The reduction of the number of accessible conformations in entangled polymer melts and in chemically crosslinked networks leads to the loss of isotropic translational motion, as presented schematically in fig. 5. Indeed, the degree of local ordering can be quantified on different time scales by various NMR techniques, using the concept of local dynamic order parameter [16,26,27], defined as $S_i(t) = \frac{1}{2}(3 \cos^2 \theta(t) - 1)$, where $\theta(t)$ describes the angle between a local chain axis and the director.

Rigid endblocks in heterogeneous triblock copolymers are another type of physical crosslinks. They result from the formation of nanodomains with different solidification temperatures [28]. In PEO-*b*-PDMS-*b*-PEO both chain ends of the flexible PDMS block are anchored to rigid, glassy PEO blocks. Similar triblock copolymers were studied before by calorimetric techniques, yet not with respect to local ordering [29]. It was observed experimentally by Fredericksen *et al.* [30] and later on by simulations [10,11] that in such systems elongated chain conformations are favored. Indeed, recent NMR investigations on amorphous PS-*b*-PB-*b*-PS triblock copolymers revealed that local order in heterogeneous block copolymers is considerably larger and longer-lived than what is found in entangled homopolymer melts. Order parameters are increased by 150% for diblock copolymers and even 200% for triblock copolymers [26]. These findings were taken as evidence for considerable stabilization of the nanoscopic order.

In this study we show that the PDMS moiety in triblock copolymers crystallizes much more easily than in the blend. We suggest that this may be related to preordering of the triblock copolymer chains while still in the molten state, according to the scenario described above, in agreement with recent findings [31,32]. Similarly, Hsu *et al.* [33] described the facilitation of structural evolution during crystallization by strongly interacting chains.

To conclude, we observed that crystallization is significantly enhanced by the presence of different types of crosslinks. We attribute the findings to substantial local chain ordering in the melt that facilitates conformational rearrangements necessary for crystallization. Although the origin of chain ordering for each of the different types of crosslinks might differ in detail, the outcome is similar.

* * *

We thank Z.-R. ZHANG, T. WAGNER and Y. YAGEN for their help. The PEO 2k was kindly provided by Clariant AG. TD acknowledges the MINERVA foundation, and thanks M. WILHELM for his support. RY-R and MG gratefully acknowledge the BSF Foundation grant no. 2000124.

REFERENCES

- [1] ARMISTEAD K. and GOLDBECK-WOOD G., *Adv. Polym. Sci.*, **100** (1992) 219.
- [2] MANDELKERN L., in *Crystallization of Polymers* (McGraw Hill, New York) 1994.
- [3] EBENGOU R. H. and COHEN-ADDAD J. P., *Polymer*, **35** (1994) 2962.
- [4] HECK B., HUGEL T., IJIMA M. and STROBL G., *Polymer*, **41** (2000) 8839.
- [5] STROBL G., *Eur. Phys. J. E*, **3** (2000) 165.
- [6] TERRILL N. J., FAIRCLOUGH P. A., TOWNS-ANDREWS E., KOMANSCHKE B. U., YOUNG R. J. and RYAN A. J., *Polymer*, **39** (1998) 2381.
- [7] OLMSTED P. D., POON W. C. K., MCLEISH T. C. B., TERRILL N. J. and RYAN A. J., *Phys. Rev. Lett.*, **81** (1998) 373.
- [8] FERRY J. D., *Viscoelastic Properties of Polymers*, 3rd edition (Wiley, New York) 1980.
- [9] GRAESSLEY W. W., *Adv. Polym. Sci.*, **47** (1982) 67.
- [10] BINDER K. and FRIED H., *Macromolecules*, **26** (1993) 6878.
- [11] MURAT M., GREST G. S. and KREMER K., *Macromolecules*, **32** (1999) 595.
- [12] BASCHNAGEL J. and BINDER K., *Macromolecules*, **28** (1995) 6808.
- [13] STARR F. W., SCHRODER T. B. and GLOTZER S. C., *Phys. Rev. E*, **64** (2001) 051503-1.
- [14] FETTERS L. J., LOSHE D. J. and GRAESSLEY W. W., *J. Polym. Sci. Part B. Polym. Phys.*, **37** (1999) 1023.
- [15] RATHGEBER S., WILLNER L., RICHTER D., BRULET A., FARAGO B., APPEL M. and FLEISCHER G., *J. Chem. Phys.*, **110** (1999) 10171.
- [16] COHEN-ADDAD J. P., *J. Chem. Phys.*, **63** (1975) 4880.
- [17] ENGLISH A. D., INGLEFIELD P. T., JONES A. A. and ZHU Y., *Polymer*, **39** (1998) 309.
- [18] GRAF R., RHEUER A. and SPIESS H. W., *Phys. Rev. Lett.*, **80** (1998) 5738.
- [19] MATHOD V. F. (Editor), *Calorimetry and Thermal Analysis of Polymers* (C. Hanser, Munich) 1994.
- [20] We used a Mettler Toledo Thermal Analysis System TA8000.
- [21] ADAM M., LAIREZ D., KARPASAS M. and GOTTLIEB M., *Macromolecules*, **30** (1997) 5920.
- [22] ZHANG Z.-R. and GOTTLIEB M., to be published.
- [23] ARANGUREN M. I., *Polymer*, **39** (1998) 4879.
- [24] LIU S. L., CHUNG T. S., OIKAWA H. and YAMAGUCHI A., *J. Polym. Sci., Part B. Polym. Phys.*, **38** (2000) 3018.
- [25] The effect of the cooling rate on the crystallization of PDMS was investigated in a different study (DOLLASE T. *et al.*, *Effect of interfaces on the crystallization behavior of PDMS*, to be published in *Interface Science*). We found that under isothermal conditions crystallization is observed at $T \leq -60^\circ\text{C}$.
- [26] DOLLASE T., GRAF R., HEUER A. and SPIESS H. W., *Macromolecules*, **34** (2001) 298.
- [27] DEMCO D. E., HAFNER S., FULBER C., GRAF R. and SPIESS H. W., *J. Chem. Phys.*, **105** (1996) 11285.
- [28] BATES F. S., *Science*, **251** (1991) 898.
- [29] SHIN H.-Y., KUO W. F., PEARCE E. M. and KWEI T. K., *Polym. Adv. Tech.*, **6** (1995) 413.
- [30] ALMDAL K., ROSEDAKE J. H., BATES F. S., WIGNALL G. D. and FREDERICKSON G. H., *Phys. Rev. Lett.*, **65** (1990) 1112.
- [31] ZHU L. *et al.*, *Macromolecules*, **34** (2001) 1244.
- [32] CHEN H.-L., HSIAO S.-C., LIN T.-L., YAMAUCHI K., HASEGAWA H. and HASHIMOTO T., *Macromolecules*, **34** (2001) 671.
- [33] HEINTZ A. M., to be published in *Macromolecules*, **35** (2002).